# RecA requires two molecules of Mg$^{2+}$ ions for its optimal strand exchange activity *in vitro*

**Raeyeong Kim[1], Shuji Kanamaru[2,3], Tsutomu Mikawa[4], Chantal Prévost[5], Kentaro Ishii[6], Kentaro Ito[2,3], Susumu Uchiyama[6,7], Masayuki Oda[8], Hiroshi Iwasaki[2,3], Seog K. Kim[1] and Masayuki Takahashi[2,*]**

[1]Department of Chemistry, Yeungnam University, Gyeonsan-city 38541, Republic of Korea, [2]School of Life Science and Technology, Tokyo Institute of Technology, 2-12-1 Ookayama, Meguro-ku, Tokyo 152-8550, Japan, [3]Institute of Innovative Research, Tokyo Institute of Technology, 2-12-1, Ookayama, Meguro-ku, Tokyo 152-8550, Japan, [4]RIKEN Quantitative Biology Center, 1-7-22 Suehiro-cho, Tsurumi-ku, Yokohama 230-0045, Japan, [5]Laboratoire de Biochimie Théorique, UPR9080 CNRS Institut de Biologie Physico-Chimique, 13 rue Pierre et Marie Curie, 75005 Paris, France, [6]Okazaki Institute for Integrative Bioscience, National Institutes of Natural Sciences, 5-1 Higashiyama, Myodaiji, Okazaki 444-8787, Japan, [7]Department of Biotechnology, Graduate School of Engineering, Osaka University, 2-1 Yamadaoka, Suita 565-0871, Japan and [8]Graduate School of Life and Environmental Sciences, Kyoto Prefectural University, 1–5 Hangi-cho, Shimogamo, Sakyo-ku, Kyoto 606-8522, Japan

## ABSTRACT

**Mg$^{2+}$ ion stimulates the DNA strand exchange reaction catalyzed by RecA, a key step in homologous recombination. To elucidate the molecular mechanisms underlying the role of Mg$^{2+}$ and the strand exchange reaction itself, we investigated the interaction of RecA with Mg$^{2+}$ and sought to determine which step of the reaction is affected. Thermal stability, intrinsic fluorescence, and native mass spectrometric analyses of RecA revealed that RecA binds at least two Mg$^{2+}$ ions with $K_D \approx 2$ mM and 5 mM. Deletion of the C-terminal acidic tail of RecA made its thermal stability and fluorescence characteristics insensitive to Mg$^{2+}$ and similar to those of full-length RecA in the presence of saturating Mg$^{2+}$. These observations, together with the results of a molecular dynamics simulation, support the idea that the acidic tail hampers the strand exchange reaction by interacting with other parts of RecA, and that binding of Mg$^{2+}$ to the tail prevents these interactions and releases RecA from inhibition. We observed that binding of the first Mg$^{2+}$ stimulated joint molecule formation, whereas binding of the second stimulated progression of the reaction. Thus, RecA is actively involved in the strand exchange step as well as bringing the two DNAs close to each other.**

## INTRODUCTION

Homologous recombination involves strand exchange between two DNAs with identical or similar sequences. This reaction plays important roles in the repair of double-strand breaks and collapsed replication forks (1–3), and is conserved in all living organisms, including some viruses. As an error-free repair process, it is important for genome stability and survival of individual organisms. In addition, the reaction promotes genomic diversity, e.g. by enabling the integration of external DNA into chromosomal DNA (4,5). In eukaryotes, homologous recombination occurs frequently during meiosis, and mixes maternal and paternal genetic information to increase genetic diversity (1–3). Both impaired and excessive homologous recombination can increase cancer risk in humans (6,7). In addition to its biological importance, the reaction has been exploited in biotechnological and medical applications such as gene therapy (8).

The RecA family protein plays a crucial role in this reaction by pairing two DNAs with identical or very similar sequences and promoting strand exchange between them (2,9,10). The canonical RecA from *Escherichia coli* has been extensively studied. *E. coli* RecA first binds to a single-stranded region of DNA (ssDNA region) created by an exonuclease. This binding is highly cooperative (11), resulting in formation of a long filament of DNA/RecA complex, termed the presynaptic complex. The RecA–ssDNA filament then binds a double-stranded DNA (dsDNA), finds a homologous sequence within the dsDNA, and then replaces one strand of the dsDNA with the ssDNA (strand exchange). The molecular mechanism of the reaction has

---

been investigated in detail (for reviews: 2,12–15), but has not yet been completely elucidated. For example, it remains unclear whether RecA solely serves to bring two DNAs close to each other, or instead promotes strand exchange more actively by repositioning the DNA strands. Precise elucidation of the mechanism is challenging because the reaction is complex and differs in many ways from conventional enzymatic reactions, e.g. rather than a small-molecule substrate, the reaction involves a long nucleoprotein filament containing many RecA molecules, and promotes strand exchange of very long DNAs (hundreds of bases).

In this study, we sought to obtain insight into the mechanism of the strand exchange reaction by elucidating the mechanism of activation by $Mg^{2+}$. *In vitro* studies showed that the RecA-promoted DNA strand exchange reaction is strongly stimulated by relatively high concentrations of $Mg^{2+}$ (5–10 mM) (9,10,16,17). Cox and colleagues observed that deletion of the C-terminal acidic tail of RecA, where several negatively charged residues are clustered, enables RecA to promote strand exchange at lower concentrations of $Mg^{2+}$ and makes the reaction almost insensitive to $Mg^{2+}$ concentration (17). They proposed that, in the absence of $Mg^{2+}$, the negative charges in the acidic tail interact with the second DNA-binding site of RecA. Binding of $Mg^{2+}$ neutralizes the negative charges and abolishes the interaction with the second DNA-binding site, making it accessible to the second DNA. Thus, $Mg^{2+}$ facilitates the binding of the second DNA and stimulates the strand exchange reaction.

We tested this hypothesis experimentally by examining whether (i) $Mg^{2+}$ indeed stimulates the reaction via binding to RecA, (ii) $Mg^{2+}$ binds at the acidic tail of RecA and (iii) $Mg^{2+}$ facilitates the binding of the second DNA to the RecA–ssDNA filament (i.e. joint molecule formation). The first point had to be addressed because other factors in the strand exchange reaction (DNA and ATP) can bind $Mg^{2+}$ (18), and such interactions might also stimulate the reaction. For this purpose, we investigated whether RecA binds $Mg^{2+}$ in the absence of DNA and ATP and estimated the binding affinity. We studied the RecA/$Mg^{2+}$ interaction by measuring changes in the thermal stability, fluorescence, and circular dichroism (CD) signals of RecA upon addition of $Mg^{2+}$. Protein thermal stability measurements are frequently used in drug discovery to search for small ligands that bind a target protein (19). Using this approach, the binding constant could be estimated by analyzing the variation in thermal stability with ligand concentration. Fluorescence and CD measurements can detect subtle structural changes in protein upon binding of a ligand (20,21). Thus, we could detect $Mg^{2+}$ binding and determine the binding constant at a given temperature. We also verified $Mg^{2+}$ binding more directly by native mass spectrometry (22,23).

The same experiments were then carried out on RecA without the C-terminal acidic tail (RecA ΔC-tail) to determine whether $Mg^{2+}$ binds in this region, as proposed by Cox and colleagues (17). If so, we would expect no $Mg^{2+}$ binding following deletion of the tail. Finally, we performed the strand exchange reaction under almost the same conditions and investigated whether the concentration of $Mg^{2+}$ required to activate strand exchange corresponds to the

binding affinity of the RecA/$Mg^{2+}$ interaction, and sought to determine which reaction step is stimulated by $Mg^{2+}$.

Our analyses support the proposal of Cox and colleagues that RecA binds $Mg^{2+}$ via its acidic tail, and that this binding stimulates joint molecule formation. In addition, we observed that RecA binds two $Mg^{2+}$ molecules, and that the binding of the second $Mg^{2+}$ stimulates another step: the progression (or completion) of strand exchange. These results suggest that RecA actively promotes the displacement and repositioning of DNA strands for strand exchange, as well as bringing the two DNAs close to each other.

## MATERIALS AND METHODS

### Materials

Wild-type full-length RecA protein (RecA) from *Escherichia coli* was purified as described in (24). The *recA* gene was cloned into a His-smt3 fusion protein expression vector, a gift from Dr. T.-F. Wang. RecA fused to His-tag SUMO protein was expressed in BL21-RIPL cells induced with IPTG (0.5 mM) and cultured overnight at 20°C. The protein was bound to a $Ni^{2+}$ column and released by cleaving the His-tag SUMO moiety with SUMO protease (Ulp1 403–621 = Ulp1 [CTD]). RecA ΔC-tail (deletion of 16 amino acids from the C-terminal end) was prepared as following. The protein was expressed in *E. coli* BL21 ΔrecA (DE3) cells transformed with the pET3a-RecA ΔC-tail vector, induced with IPTG (0.5 mM) and cultured for 5 h at 37°C. RecA ΔC-tail was then purified by using TOYOPEARL Butyl-650M column (TOSOH), P11 column (Whatman) and MonoQ 5/50 GL column (GE Healthcare).

φX174 circular ssDNA and dsDNA were purchased from New England Biolabs. The circular dsDNA was linearized by digestion with *Apa*LI restriction enzyme. Poly(dT), ATP and ATPγS were from Sigma-Aldrich. Their concentrations were determined from their UV absorption using the following molar extinction coefficients: $\varepsilon_{264\,nm} = 8520$ $M^{-1}$ $cm^{-1}$ for poly(dT); $\varepsilon_{260\,nm} = 15\,400$ $M^{-1}cm^{-1}$ for ATP and ATPγS.

### Experimental conditions

Experiments were performed in Buffer T containing 30 mM Tris/HCl (pH 7.5), 0.1 mM EDTA, 0.07% Tween-20 (Sigma), and the indicated concentrations of $Mg^{2+}$ and ATP (or ATPγS). In the text, the concentration of free $Mg^{2+}$ (after subtraction of 0.1 mM $Mg^{2+}$ chelated by EDTA) is presented without further mention. Tween-20 was present to avoid adsorption of RecA on the surface of the quartz cell or plastic tube.

### CD measurements

CD spectra were measured in a Jasco J-810 or J-820 CD spectrometer in step mode (data interval: 0.1 nm; time constant: 0.175 s; bandwidth: 2 nm). Temperature was controlled by a Peltier effect controller. A 1 × 1 cm quartz cell was used for quick mixing of added $Mg^{2+}$ with the help of magnetic stirring. This approach was taken to avoid locally

high $Mg^{2+}$ concentrations, which can promote precipitation of RecA (25). On the other hand, because the path length of the cell was 1 cm, the UV absorption of samples was too high to measure CD signals below 210 nm.

### Thermal unfolding

Thermal unfolding of RecA was assessed by monitoring the change in the CD signal at 222 nm (bandwidth, 5 nm; data interval, $0.1°$C; time constant, 2 s) upon temperature elevation ($1°$C/min). A mini-cuvette of $1 \times 0.2$ cm (Hellman) with a path length of 1 cm was used for these measurements.

### Fluorescence measurements

Fluorescence of RecA was measured in a Jasco FP-8300 fluorometer. Total fluorescence (intensity) and fluorescence anisotropy were measured at the same time using automated anisotropy measurement software (Jasco). Fluorescence from tyrosine residues was measured at 305 nm (bandwidth: 10 nm) upon excitation at 270 nm (bandwidth: 5 nm). Fluorescence from tryptophan residues was measured at 350 nm (bandwidth: 10 nm) upon excitation at 295 nm (bandwidth: 5 nm). The results of 20 measurements were averaged. Temperature was held constant using a Peltier effect controller.

### Native mass spectrometry

Native mass spectrometry was performed as described previously (26). Briefly, 30 μM full-length RecA or RecA ΔC-tail was incubated for 30 min on ice in the presence or absence of 100 μM $MgCl_2$ in Buffer T. The buffer was then replaced with 150 mM ammonium acetate (pH 6.8) by passing the samples through a MicroBioSpin-6 column (Bio-Rad). The buffer-exchanged samples were immediately analyzed on a nanoflow electrospray ionization mass spectrometer using gold-coated glass capillaries made in-house (approximately 2–5 μl of sample was loaded per analysis). Spectra were recorded on a SYNAPT G2-Si HDMS mass spectrometer (Waters) in positive-ionization mode at 1.33 kV with sampling cone voltage and source offset voltage of 150 V, trap and transfer collision energy of 0 V, and trap gas flow rate of 5 ml/min. The spectra were calibrated using 1 mg/ml cesium iodide and analyzed using the MassLynx software (Waters).

### Molecular dynamics simulation

The molecular dynamics simulation of the RecA presynaptic filament was performed based on the crystallographic structure of RecA with an ATP analog and oligo(dT) (PDB: 3CMW) (27). The acidic tail (residues 334–352), which is absent from the crystal structure due to its disordered character, was added in extended conformation using scripts written in-house. The filament was then soaked in a box with 289, 200 TIP3P water molecules. To accommodate the tails in their extended conformation, a box size of $241 \times 209 \times 186$ Å with periodic boundary conditions was required. A total of 914 $Na^+$ and 816 $Cl^-$ ions were added to reach a concentration of 0.15 mol/l after maintaining

electro-neutrality. The system was subjected to molecular dynamics simulations using the NAMD 2.10 software (28) and the CHARMM27 force field (29). Following 5000 steps of conjugate gradient energy minimization, the simulation protocol included heating to 310 K in steps of 2 K, with a 30 ns equilibration phase and a 100 ns production phase. Time steps of 2 fs were used (SHAKE algorithm). The particle-mesh Ewald method was used to account for long-range electrostatic interactions, and van der Waals interactions were smoothly switched off at 10–12 Å. Temperature and pressure were maintained throughout the simulation using a Langevin dynamics scheme and a Nosé–Hoover–Langevin piston, respectively. During equilibration, the protein Cα carbons were harmonically restrained in their initial positions, with a force constant decreasing from 0.5 to 0.05 kcal $mol^{-1}$ $Å^{-2}$, in order to allow the large solvent box to equilibrate. No restraint was applied during the production phase.

The simulation of isolated RecA protein was performed based on the structure of the central monomer from the 3CMW crystal structure as a starting point, using a $107 \times 128 \times 105$ Å solvent box filled with 44 018 water molecules, 133 $Na^+$ ions, and 124 $Cl^-$ ions. The simulation protocol was identical to that used for the filament, except that the production phase was prolonged to 150 ns. The final 50 and 100 ns of the production phase were considered in the analyses of the filament and the isolated protein trajectories, respectively.

In-house Python scripts based on the PTools library (30) were used to compute the number of contacts between different regions of the system. For each contact pair, both the contact occurrence and the persistence time of the contact were recorded.

### DNA three-strand exchange reactions

Three-strand exchange reactions were carried out in 30 mM Tris–HCl (pH 7.5), 1 mM dithiothreitol, 5% (w/v) glycerol, 2 mM ATP and the indicated concentration of $MgCl_2$. The reaction solution also contained an ATP regeneration system of 8 units/ml creatine kinase and 8 mM phosphocreatine, as described in (31). All incubations were carried out at $37°$C. The full-length wild-type RecA protein (5 μM) was pre-incubated with 10 μM (in nucleotides) φX174 circular ssDNA for 10 min. SSB protein (1 μM) was added and further incubated for 10 min. The reaction was initiated by the addition of *Apa*LI-treated φX174 linear dsDNA (10 μM in nucleotide pairs). After another 60 min of incubation, the reaction was stopped by addition of 1.2 μg of proteinase K and 1% SDS (final concentrations), incubated for an additional 15 min, and then mixed with one-tenth volume of a solution containing 0.9% SDS, 50% (w/v) glycerol and 0.05% bromophenol blue. Samples were subjected to electrophoresis for 120 min at 50 V on 1.0% agarose gels in $1\times$ TAE buffer, stained with SYBR Gold, and exposed to ultraviolet light. Gel images were digitized on a LAS-400mini image analyzer (Fujifilm), and DNA bands were quantified with Multi Gauge software, version 3.2 (Fujifilm).
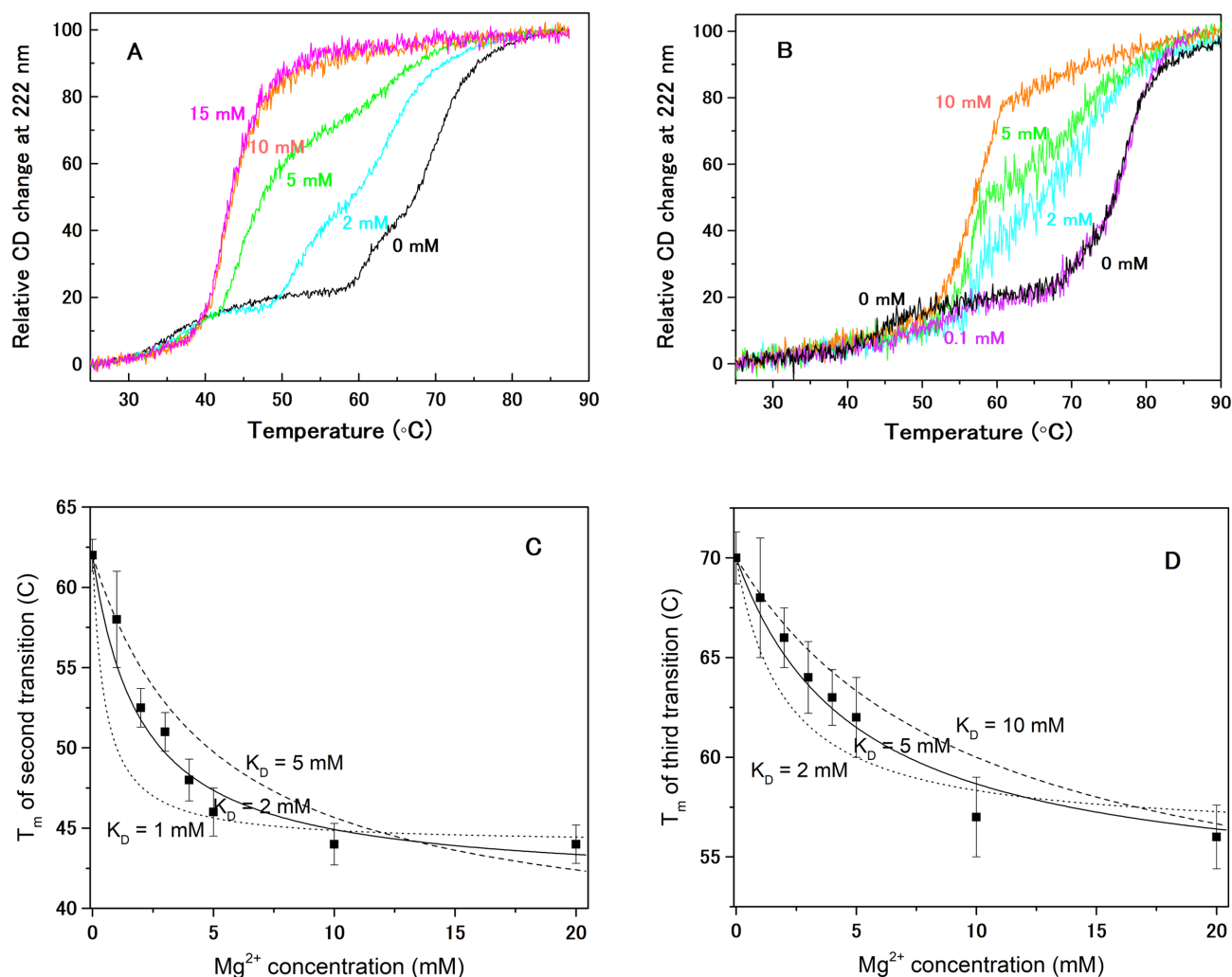
**Figure 1.** $Mg^{2+}$ ion facilitates thermal unfolding of RecA. (**A**) Thermal unfolding of 2 μM RecA with increasing temperature was followed by a change in the CD signal at 222 nm. $Mg^{2+}$ concentrations are 0 (black), 2 (cyan), 5 (green), 10 (orange) and 15 mM (magenta). (**B**) The same experiment described in A was performed for 2 μM RecA in the presence of 6 μM (in bases) poly(dT) and 50 μM ATPγS. The result for 0.1 mM $Mg^{2+}$ (magenta) is also shown. (**C**) Temperature of the second transition of full-length RecA, plotted as a function of free $Mg^{2+}$ concentration. Expected curves for various equilibrium dissociation constants ($K_D$ = 1 mM [dotted line]; 2 mM [solid line]; 5 mM [dashed line]) are shown for comparison with the experimental data. (**D**) Temperature of the third transition, plotted as in panel C. Expected curves were generated with $K_D$ = 2 mM (dotted line), 5 mM (solid line) and 10 mM (dashed line).

### Fluorescence resonance energy transfer (FRET)-based real-time measurements of DNA strand pairing and DNA strand displacement

Reaction protocols were described in (32,33). DNA substrates, 83 bases ssDNA and 40 base pair long dsDNA were identical to those used in previous paper (32) and were prepared in the same manner. The concentrations of all components are stated as their final concentrations in the reaction mixture, and those of DNA in fragment. The reactions were carried out in buffer T containing indicating $MgCl_2$ and 2 mM ATP at 37°C. In assay 1 (pairing assay), the presynaptic filament was formed by incubating 36 nM 5′ fluorescein amidite (FAM)-labeled ssDNA with 1.5 μM RecA for 5 min. The reaction was started by the addition and mixing of 36 nM 3′ carboxy-x-rhodamine (ROX)-labeled dsDNA to the presynaptic complex solution in the cuvette by pipetting. To follow the reaction, the change in fluorescence of the FAM probe was monitored at 525 nm (bandwidth: 20 nm) upon excitation at 493 nm (bandwidth: 1 nm) in an FP-8300 spectrofluorometer (JASCO) equipped with a Peltier temperature control apparatus. Data were collected every second (response time: 0.2 s). Dead time was less than 15 s. For assay 2 (standard DNA strand displacement assay), the presynaptic filament was formed as in the pairing assay, except non-labeled ssDNA was used. The reaction was initiated through the addition of 36 nM dsDNA, labeled with FAM at the 5′ end of the outgoing strand and ROX at the 3′ end of its complementary strand, to the cuvette containing the presynaptic complex solution. The reaction was monitored as described above.
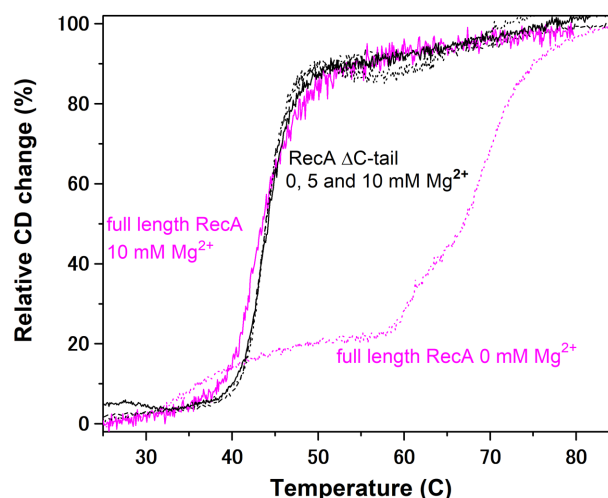
## RESULTS

### Binding of two $Mg^{2+}$ ions decreases the thermal stability of RecA

We first examined binding of $Mg^{2+}$ to RecA by monitoring changes in protein thermal stability, which is often affected by binding of ligand (19). Specifically, we assessed the thermal unfolding of RecA based on the change in the intensity of the CD signal at 222 nm, which primarily reflects alpha-helix structure (21). The thermal unfolding curve of RecA exhibited three transitions: the first at a low temperature (around 35°C), the second at 62°C, and the final at 71°C (Figure 1A). Crystallographic analysis of RecA has shown that it is composed of three domains, the N-terminal, C-terminal, and large central domains (27,34). Because each domain contains alpha-helix structures, the presence of three transitions likely reflects this three-domain structure, i.e. each transition corresponded to the unfolding of one of the domains, and each domain unfolded independently. None of the transitions was reversible, preventing a rigorous thermodynamic analysis.

The presence of $Mg^{2+}$ ions significantly decreased the temperatures of the second and third transitions, but increased that of the first (Figure 1A). The second transition was affected at lower $Mg^{2+}$ concentrations, whereas the third transition was affected at higher $Mg^{2+}$ concentrations. The effect on the second transition was saturated around 5 mM $Mg^{2+}$, with the half-maximal effect at around 2 mM, whereas the effect on the third transition required more than 10 mM $Mg^{2+}$ for saturation, with the half-maximal effect at around 5 mM (Figure 1A). Thus, RecA binds at least two $Mg^{2+}$ ions with distinct binding affinities: $K_{D1} = 2$ mM and $K_{D2} = 5$ mM. The changes in the first and third transitions probably occurred at the same time, i.e. upon binding of the second $Mg^{2+}$.

To more precisely estimate the binding affinity for each $Mg^{2+}$, we analyzed how the second and third transition temperatures varied with $Mg^{2+}$ concentration. Such an analysis could not be performed for the first transition because the change was small, and also because this transition merged with the second one at 3 mM $Mg^{2+}$. The transition temperatures were estimated at each $Mg^{2+}$ concentration by two approaches: analysis of the first derivative of the unfolding curve and the half-transition point. Both methods yielded similar temperatures, and the difference was less than 0.5°C. The half-transition temperatures were used for the analysis. The variation in the second transition could be fitted with a binding curve with $K_{D1} = 2 \pm 1$ mM (Figure 1C), and that of the third transition with a binding curve with $K_{D2} = 5 \pm 2$ mM (Figure 1D).

The change in thermal stability was not due to a simple increase in ionic strength or salt concentration. Addition of KCl did not change the stability as much as addition of $Mg^{2+}$ (Supplementary Figure S1): 100 mM KCl caused a 5°C decrease in the second and third transitions. The effect was smaller at 50 mM and even reversed at higher concentrations (500 mM). Therefore, the large change in the thermal stability observed in the experiments described above was due to a specific effect of $Mg^{2+}$.



**Figure 2.** Deletion of the acidic tail makes RecA thermal stability insensitive to $Mg^{2+}$ ion. Thermal unfolding of 2 μM RecA ΔC-tail was studied with 0 mM (dotted line), 5 mM (dashed line) and 10 mM (solid line) $Mg^{2+}$ as described in Figure 1A. All of the resultant curves are almost fully superimposed and are consequently not distinguishable. The unfolding curves of full length RecA without (purple dots) and with (purple line) 20 mM $Mg^{2+}$ are shown for comparison.

The $Mg^{2+}$-dependent destabilization of RecA occurred also when RecA was in the presynaptic filament, the RecA–ssDNA complex. The thermal folding of RecA was carried out in a complex with oligo(dT), a model ssDNA, and ATPγS, an ATP analog that is hydrolyzed very slowly. A decrease in the temperature of the second and third transitions was observed with the half-maximal effect at 1.5 and 5 mM of $Mg^{2+}$, respectively. The binding affinities of $Mg^{2+}$ to RecA in the presynaptic filament was, thus similar to the affinities to free RecA. Formation of the presynaptic complex was indicated by an overall increase in thermal stability: the first transition was at 46°C (vs. 35°C), the second at 75°C (vs. 62°C), and the third at 82°C (vs. 71°C) in the absence of $Mg^{2+}$ (cf. Figure 1A and B).

When RecA was in the presynaptic complex, binding of another $Mg^{2+}$ was observed at low concentrations. The presence of 0.1 mM $Mg^{2+}$ stabilized the first transition (from 45 to 50°C) without affecting other transitions (Figure 1B). However, 0.1 mM $Mg^{2+}$ had no effect on the thermal unfolding pattern of free RecA (not shown). The change in the first transition of RecA in the presynaptic filament probably reflects the high-affinity binding of another $Mg^{2+}$ ion at the ATP/RecA interface. A similar change was observed for RecA with ATPγS alone (Supplementary Figure S2). We conclude that $Mg^{2+}$ ions bind RecA in the presynaptic filament in a similar manner to free RecA, as well as binding to the ATP/RecA interface.

### Deletion of the C-terminal acidic tail abolishes the $Mg^{2+}$ effects

To verify that $Mg^{2+}$ binds to the C-terminal acidic tail of RecA, we studied the thermal stability of RecA ΔC-tail. No significant change was observed in the thermal stability of the RecA ΔC-tail by $Mg^{2+}$ (Figure 2), supporting the
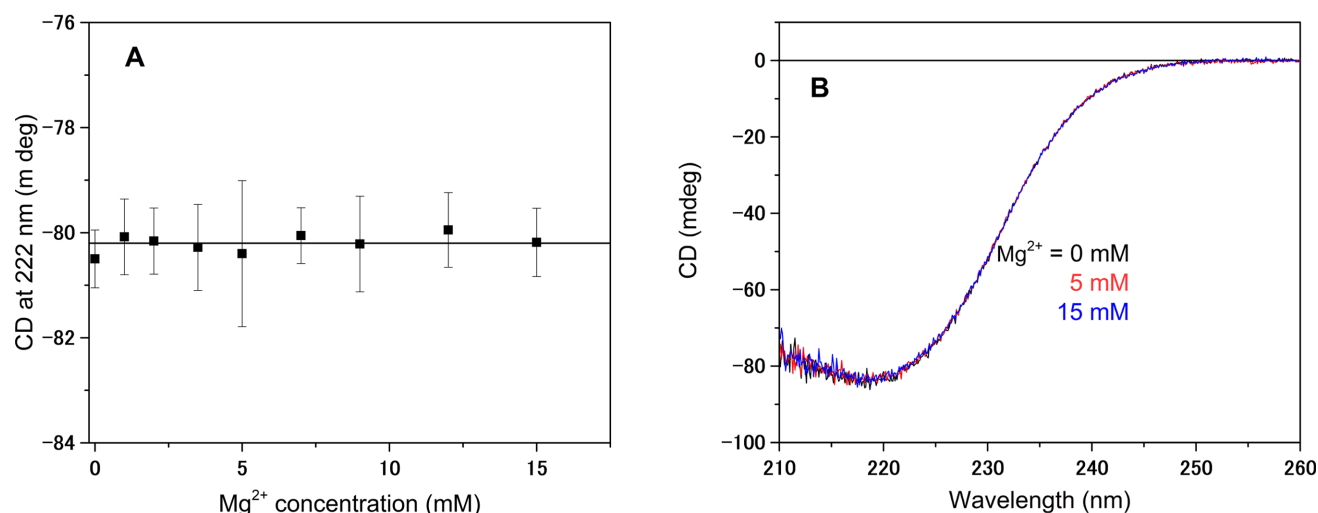
**Figure 3.** $Mg^{2+}$ ion causes no change in the CD signal of RecA. (**A**) CD signal intensity at 222 nm of 2 $\mu$M RecA, plotted as a function of $Mg^{2+}$ concentration. (**B**) CD spectra of 2 $\mu$M RecA in the presence of 0 mM (black), 5 mM (red) and 15 mM (blue) $Mg^{2+}$ are shown. All curves are superimposed and not distinguishable.

proposition of Cox and colleagues that the tail binds $Mg^{2+}$ ([17]). Furthermore, the thermal unfolding curve was similar to that of full-length RecA in the presence of 20 mM $Mg^{2+}$, the saturating concentration. In other words, the binding of $Mg^{2+}$ exerted the same effect as deletion of the acidic tail. This is consistent with the idea that the tail interacts with other part(s) of RecA via its negative charged residues, but neutralization of these charges by $Mg^{2+}$ abolishes these interactions and decreases the thermal stability of the protein.

### $Mg^{2+}$ does not affect the folding pattern of RecA

To determine whether the decrease in RecA thermal stability is due to a modification of its folding pattern, we measured the CD signal. The CD signal at 222 nm, which is primarily related to the alpha-helix structure ([21]), was unchanged upon addition of $Mg^{2+}$ at a low temperature, 20°C (Figure 3A). Similarly, the CD spectral shape in the far-UV region was not at all altered upon addition of $Mg^{2+}$ up to 15 mM (Figure 3B). Thus, $Mg^{2+}$ did not affect the secondary structure, i.e., the folding pattern of RecA, suggesting that the decrease in thermal stability was due to changes in its tertiary structure (i.e. domain/domain contacts) or subunit/subunit contacts.

### Fluorescence analysis detects binding of $Mg^{2+}$ ions to RecA

Next, we investigated the binding of $Mg^{2+}$ and the resulting structural change in RecA by monitoring the fluorescence change of RecA upon addition of $Mg^{2+}$. Because fluorescence is very sensitive to changes in a residue's local environment, measurement of this feature can reveal changes in the tertiary and quaternary structures of a protein ([20]). In contrast to the thermal stability analysis, fluorescence measurement enabled us to study binding of $Mg^{2+}$ to the native form of RecA at a given temperature. Hence, these experiments were carried out at 20°C, a temperature at which RecA exists in its native form. RecA contains two tryptophan residues and seven tyrosine residues ([35]), none of

which are in the acidic tail. The two tryptophan and three tyrosine residues are in the C-terminal domain, whereas four tyrosine residues are in the central domain ([27,32]). Tryptophan and tyrosine fluorescence were observed separately by selection of appropriate excitation and emission wavelengths ([20]).

Upon addition of $Mg^{2+}$, tryptophan fluorescence decreased slightly (about 10% in intensity) (Figure 4A), but no such change was observed for RecA $\Delta$C-tail. The change in fluorescence intensity with $Mg^{2+}$ fit closely to a curve generated by a model in which two $Mg^{2+}$ ions bind with $K_{D1}$ = 2 mM and $K_{D2}$ = 5 mM, with the assumption that the first binding does not affect intensity. Because the measurements were performed at 20°C, whereas the binding constants were estimated around the unfolding temperature in the thermal stability experiments, these results indicate that the binding constants are not especially sensitive to temperature, and that $Mg^{2+}$ ions bind to the native form of RecA. This observation excludes the possibility that $Mg^{2+}$ binds mainly to unfolded RecA and thereby promotes its destabilization. The small magnitude of the fluorescence change indicates that the environment of the two tryptophan residues did not undergo a large change.

By contrast, no significant change (<5%) was observed in tyrosine fluorescence upon addition of $Mg^{2+}$ (Figure 4B). Thus, either $Mg^{2+}$ binding does not affect the environment of any tyrosine residue, or (given that there are so many tyrosines) the potential change in fluorescence intensity of one of the tyrosines is masked or compensated by the fluorescence of another.

We then performed fluorescence anisotropy measurements, which are related to the local motion of tryptophan and tyrosine residues ([20]). Large anisotropy values (>0.2) indicate an absence of quick (nanosecond-scale) local motion. The fluorescence anisotropy of tryptophan residues was 0.10, indicating some local motion, and was not affected by $Mg^{2+}$. By contrast, that of tyrosine residues increased from 0.163 to 0.183 (Figure 4C and D), indicating
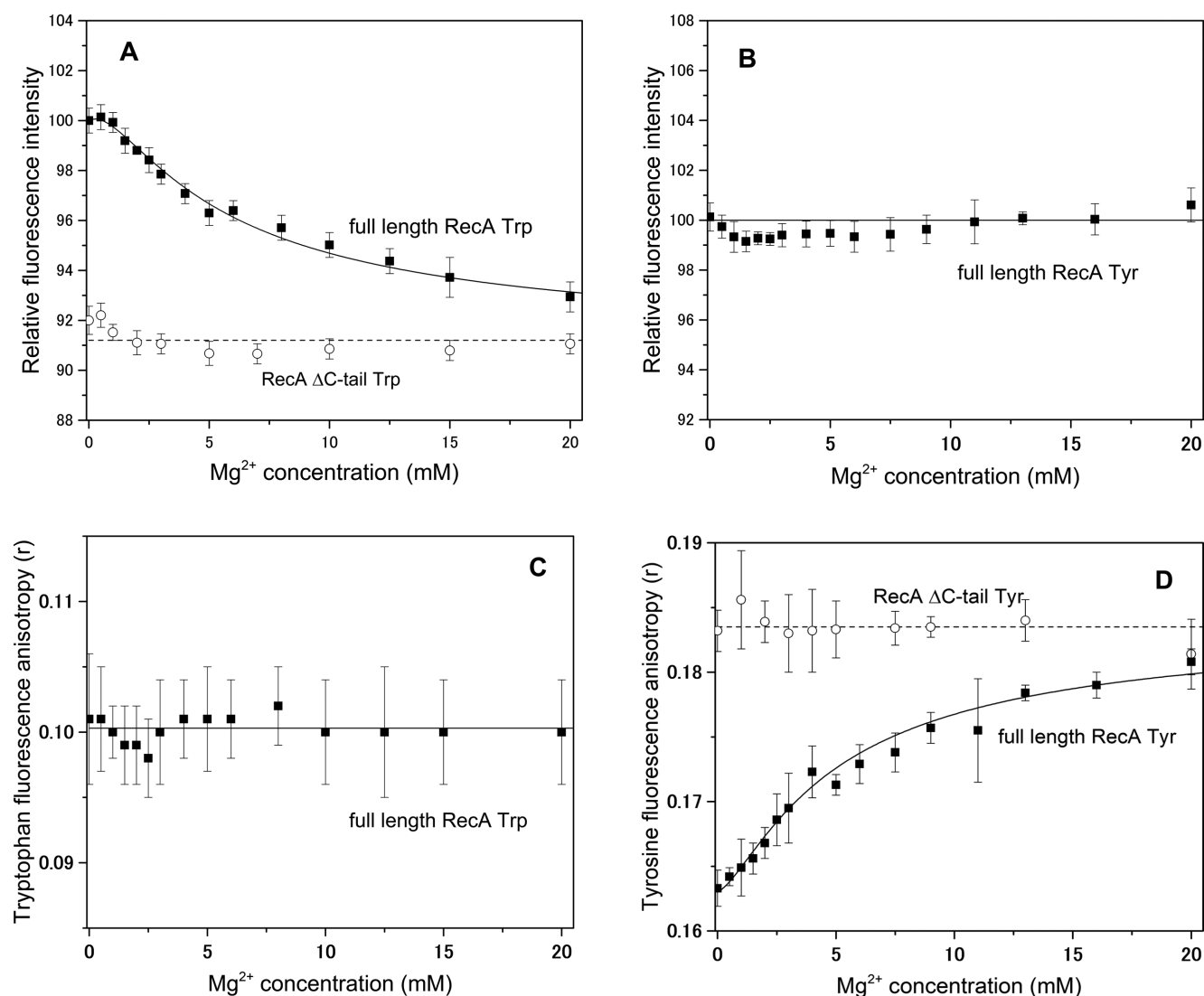
**Figure 4.** $Mg^{2+}$ ion affects the fluorescence intensity and fluorescence anisotropy of RecA. Fluorescence intensity (**A**, **B**) and anisotropy (**C**, **D**) of tryptophan (A, C) and tyrosine (B, D) residues of RecA were measured at various $Mg^{2+}$ concentrations and plotted. In A, the tryptophan fluorescence intensity of RecA without its acidic tail is plotted with open symbols. In D, the fluorescence anisotropy of tyrosine residues of RecA without its acidic tail is plotted with open symbols. A theoretical binding curve was generated based on assumptions that RecA binds two $Mg^{2+}$ ions with $K_{D1} = 2$ and $K_{D2} = 5$ mM, and that no signal change occurs upon binding of the first $Mg^{2+}$.

some structural change in RecA that likely prevents the motion of one tyrosine-spanning loop. Again, the experimental data fit closely to a model in which two $Mg^{2+}$ ions bound with $K_{D1} = 2$ mM and $K_{D2} = 5$ mM, with the assumption that the first binding does not affect the anisotropy value. These observations are consistent with the results of the thermal unfolding study and the fluorescence analysis of tryptophan residues. The structural change occurred largely upon binding of the second $Mg^{2+}$. The fluorescence anisotropy of tyrosine residues of RecA ΔC-tail was not affected by $Mg^{2+}$, and was similar to that of full-length RecA in the presence of saturating concentration of $Mg^{2+}$.

**Native mass spectrometry detects binding of more than two $Mg^{2+}$ ions by RecA**

To more directly verify the binding of two $Mg^{2+}$ ions by RecA, we performed native mass spectrometric analysis. This technique is a powerful tool for studying the stoichiometry of protein–ligand interactions by determining the masses of complexes (25,26). In native mass spectrometric analysis, which is performed in the vacuum environment, ionic interaction is stronger than in water (36). Therefore, the measurements were made at low ion concentration to exclude non-specific binding. The spectrum of full-length RecA exhibited an ion series indicating the presence of monomer, dimer, trimer, and tetramer forms with masses of 37, 844, 75, 677, 113, 518 and 151, 359 Da, respectively (Supplementary Figure S3, top). In the expansion of the +12 peak of the monomeric RecA, one major
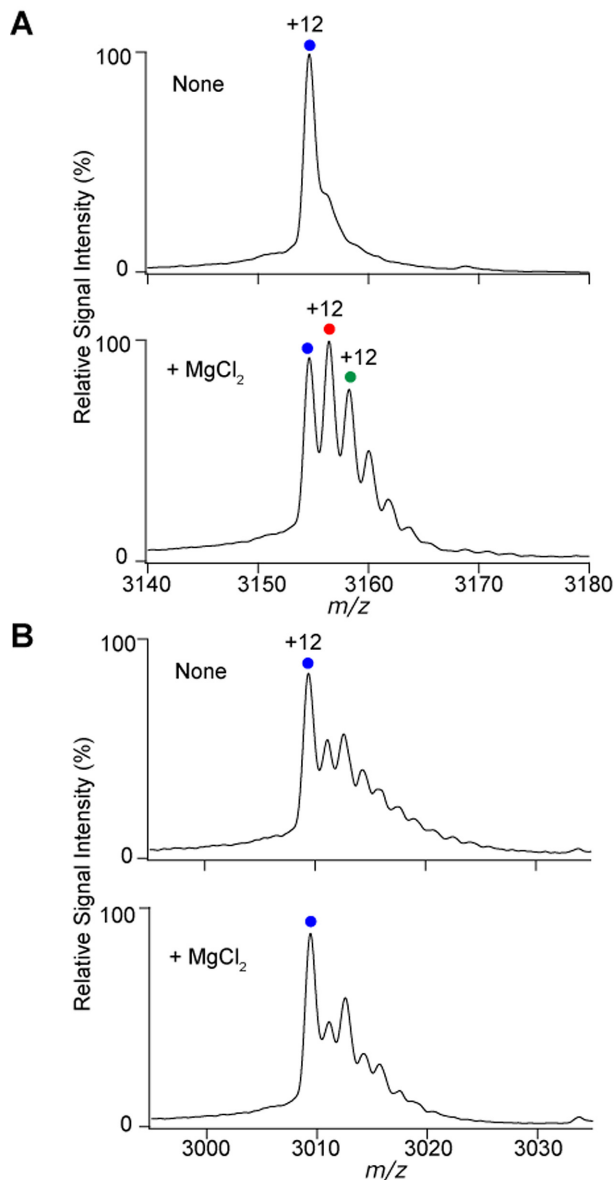
**Figure 5.** Mass spectra of full-length and acidic tail–deleted RecA, with or without MgCl$_2$. (**A**) Expansion of the +12 peak of the monomeric RecA spectra in the absence (top) and presence (bottom) of 100 μM MgCl$_2$. Blue, red, and green circles show the ion series of RecA without Mg$^{2+}$, with one Mg$^{2+}$ ion, and with two Mg$^{2+}$ ions, respectively. (**B**) Expansion of the +12 peak of the monomeric form of RecA ΔC-tail in the absence (top) and presence (bottom) of 100 μM MgCl$_2$. Blue circles show the protein with no ion.

and one minor peak were observed, corresponding to RecA (37, 844 Da) without any bound ion and RecA with an NH$_4^+$ or Na$^+$ adduct (37 862 Da; Figure 5A). In the presence of MgCl$_2$, the spectrum of monomeric RecA exhibited an ion series indicating the presence of RecA without Mg$^{2+}$ (37 843 Da), with one Mg$^{2+}$ (37 864 Da), with two Mg$^{2+}$ (37 886 Da), and with more Mg$^{2+}$ (Figure 5A). The spectrum of RecA ΔC-tail exhibited an ion series indicating the presence of monomer, dimer, trimer, and tetramer forms (Supplementary Figure S3, bottom), like that of full-length RecA. The spectrum of the monomeric form of RecA ΔC-

tail presented several peaks, corresponding to RecA ΔC-tail without any bound ion and one, two and more K+ adducts. However, the spectrum was obviously unchanged by the addition of MgCl$_2$ (Figure 5B). This observation supports the idea that RecA can bind at least two Mg$^{2+}$ ions with its acidic tail. A larger proportion of ion adduct forms in RecA ΔC-tail compared to in full length RecA may be due to difference in protein preparation and storage conditions.

**Molecular modeling supports the dynamic interaction of the acidic tail with other parts of RecA**

We then performed molecular simulation to investigate the possibility of an interaction between the disordered C-terminal acidic tail and the structured part of the RecA protein (protein core). All-atom molecular dynamics simulations of the 3D structure of RecA, determined by X-ray crystallography (27), were performed in a solvated environment with a physiological ionic concentration. Because the structure of the acidic tail has not been determined by X-ray crystallography (27,34), we attached the acidic tail in an extended conformation pointing away from the proteins. Simulations were performed on an isolated RecA (150 ns) and on RecA in a presynaptic filament consisting of seven monomers of RecA with ssDNA and ATP (i.e. more than one turn of the helix). In the second case, seven independent RecA proteins containing their acidic tails were simultaneously simulated, increasing the extent of conformational space sampled by the tails. In both cases, the acidic tails rapidly folded into unstable, mostly coiled states. The number of interactions between the tails and the filament cores, defined as the number of pairs of atoms of each component closer than 3 Å, reached a plateau after about 50 ns in both the monomer and oligomer cases. The initial 50 ns simulations were ignored in subsequent analysis. Although the interactions between the protein cores and acidic tails were mostly transient, with persistence times rarely reaching 20 ns, monitoring of the frequency of interactions for each amino acid revealed a pattern of preferred interaction regions on the core protein (Figure 6). The simulation predicted that the tail residues (334–352) interacted with the C-terminal (270–333), N-terminal (1–37), and central domains of RecA, although these interactions were distributed differently for isolated RecA versus RecA in the filament. In the filament, the tail also interacted with residues of the neighboring protein core, suggesting that this region influences subunit/subunit contact. No interactions were observed involving Arg226, Lys245, Arg227 or Arg243, which are considered to be within the second DNA-binding site (14,27). By contrast, we did observe an interaction with the residues in the second DNA entrance (gateway) (37,38).

**Mg$^{2+}$ stimulates both binding of the second DNA and progression of strand exchange**

Finally, we examined the effect of Mg$^{2+}$ on RecA-promoted strand exchange reaction under similar conditions. Specifically, we investigated whether the Mg$^{2+}$ concentrations required to activate strand exchange corresponded to the Mg$^{2+}$-binding affinity of RecA and whether binding of the first Mg$^{2+}$ was sufficient to activate RecA or the binding of two Mg$^{2+}$ was required.
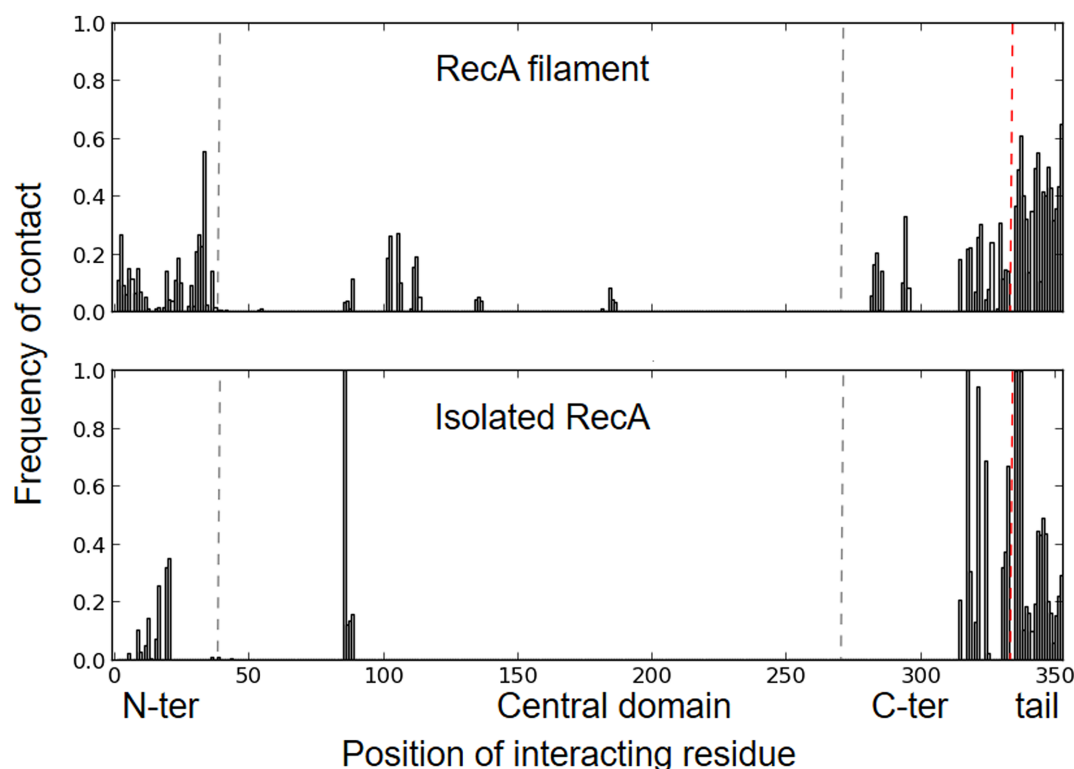
**Figure 6.** Contacts between the RecA core and the C-terminal tail. Frequency of contacts between amino acids 1–332 from the RecA protein core and amino acids 334–352 from the acidic tail during (top) 50 ns MD simulation of a seven-monomer filament (results averaged over the seven monomers) and (bottom) 100 ns MD simulation of an isolated RecA protein. Two amino acids were considered to be in contact if any of their atoms were closer than 3 Å. Vertical dashed black lines indicate the borders between the central domain and the N-terminal (left) and C-terminal (right) domains. The red dashed line indicates the starting residue of the acidic tail (residue 333).

The strand exchange reaction was performed between one circular ssDNA and one linear dsDNA. The reaction was stopped after 60 min of incubation, and the products were separated by gel electrophoresis and quantified. In this experiment, the intermediate (joint molecules) and the final product (nicked circular dsDNA) could be quantified separately (31), enabling a rough determination of which step of the reaction was stimulated by $Mg^{2+}$.

Stimulation of final product formation, i.e. the completion of the reaction, reached a plateau at around 12 mM $Mg^{2+}$, with the half-effect at 5.8 mM (Figure 7A). By contrast, the maximum appearance of intermediate molecules was achieved at 6 mM $Mg^{2+}$, with the half-effect at 3 mM $Mg^{2+}$ (Figure 7A). Because the strand exchange experiments were performed in the presence of 2 mM ATP, which interacts with $Mg^{2+}$ with millimolar affinity, these results indicate that half-maximal stimulation of the joint molecule formation occurred at around 2 mM free $Mg^{2+}$, and that of reaction completion at around 5 mM free $Mg^{2+}$. Thus, binding of one $Mg^{2+}$ ion is probably sufficient to stimulate joint molecule formation, whereas two $Mg^{2+}$ ions are required to stimulate reaction completion.

To further confirm the conclusion, we observed the reaction kinetics in real time at various $Mg^{2+}$ concentrations. We used FRET-based strand exchange assay (32,33): two of the three DNA strands involved in the reaction were labelled by appropriate fluorescence dyes, FAM and ROX, at their end. In assay 1, the binding of dsDNA to the RecA/ssDNA complex, which promotes FRET, is detected by decreases in intensity of FAM fluorescence. In assay 2, the separation of DNA strands from dsDNA (DNA strand displacement), which abolishes the FRET, is detected by increase in intensity of FAM fluorescence. The second observation corresponds to the reaction completion while the first one to biding of second DNA. We measured, in both cases, the initial velocity. The results indicate that half-maximal stimulation of the paring formation occurred at ∼3 mM $Mg^{2+}$ (Figure 7B), and that of reaction completion at ∼7.5 mM $Mg^{2+}$ (Figure 7C), confirming the conclusion that biding of one $Mg^{2+}$ is enough to stimulate pairing step while binding of two $Mg^{2+}$ is required for reaction completion.

## DISCUSSION

In this study, we investigated how $Mg^{2+}$ stimulates the RecA-promoted strand exchange reaction, with the goal of obtaining insight into the mechanism of the strand exchange reaction itself. We observed binding of two $Mg^{2+}$ ions at the C-terminal tail, and discovered that RecA plays a role in the progression of the strand exchange reaction, as well as joint molecule formation. In addition, we experimentally demonstrated that the acidic tail of RecA exerts a negative effect on the reaction.

First, we examined the proposition of Cox and colleagues (17) that RecA binds $Mg^{2+}$ at the acidic tail, which interacts via its charged residues with the second DNA-binding
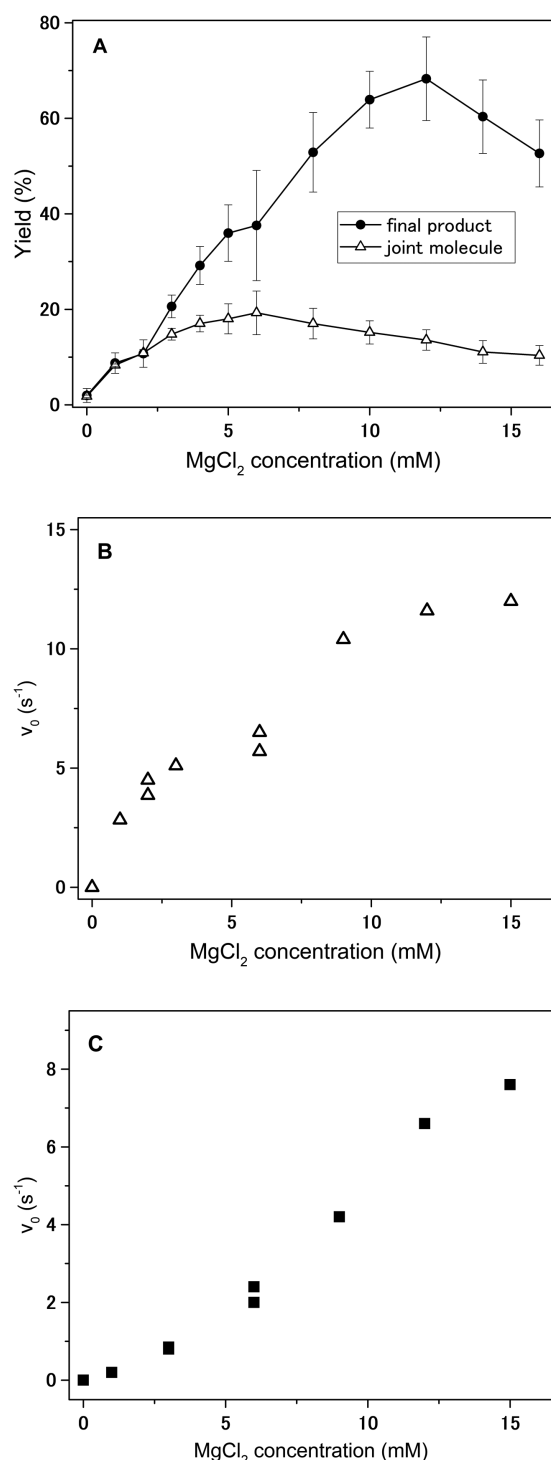
**Figure 7.** $Mg^{2+}$ ion stimulates both joint molecule formation and completion of the strand exchange reaction by RecA. (**A**) DNA strand exchange between a circular single-stranded DNA (concentration) and linear double-stranded DNA (concentration) was performed in the presence of 5 μM RecA, 2 mM ATP, and the indicated concentrations of $Mg^{2+}$. After electrophoretic separation of the products, the bands corresponding to the joint molecule (triangles) and the final product (circles) were quantified and plotted as a function of $Mg^{2+}$ concentration. (**B**) FRET-based strand exchange assay was performed at various $Mg^{2+}$ concentrations for real time observation of reaction kinetics. Initial velocity of paring is presented in a function of $Mg^{2+}$ concentration. (**C**) Initial velocity of strand displacement is presented in a function of $Mg^{2+}$ concentration.

site. In this model, binding of $Mg^{2+}$ abolishes this interaction, allowing access of the second DNA to the second DNA-binding site, thereby stimulating the strand exchange reaction. We observed the binding of $Mg^{2+}$ to free RecA without DNA or ATP by monitoring changes in the thermal stability and fluorescence characteristics of the protein. The results revealed that RecA binds two $Mg^{2+}$ ions with an affinity of 2 and 5 mM. This affinity corresponds closely to the $Mg^{2+}$ concentrations required to stimulate the strand exchange reaction, supporting the idea that $Mg^{2+}$ stimulates the reaction by binding to RecA. We also observed that deletion of the C-terminal acidic tail caused all characteristics of RecA to become insensitive to $Mg^{2+}$ and similar to those of the full-length protein in the presence of saturating $Mg^{2+}$. This supports the proposal of Cox and colleagues (17) that the acidic tail hampers the strand exchange reaction in the absence of $Mg^{2+}$, probably by interacting with other parts of RecA. The binding of $Mg^{2+}$ to the tail prevents such interactions in a similar way to deletion of the acidic tail, enabling the strand exchange reaction to occur. Molecular dynamics analysis of the acidic tail further supported this idea.

However, our simulation did not show an interaction of the acidic tail with the second DNA-binding site. Therefore, we did not obtain direct support for the hypothesis that the tail directly interacts with the second DNA-binding site and hampers the reaction. By contrast, our analysis revealed interactions of the tail with Lys6, Lys8, Lys19 and Lys23 of the N-terminal domain, which are important for non-specific binding of the second DNA (14), as well as with the C-terminal domain, which contains the gateway for the incoming dsDNA (37,38). The binding of $Mg^{2+}$ probably attenuates the interactions with these residues or simply masks the negative charges of RecA, thereby facilitating the approach of the second DNA.

Our analyses showed that RecA binds two $Mg^{2+}$ ions on its C-terminal acidic tail, and that binding of the second $Mg^{2+}$ ion is important for stimulating the progression of strand exchange, whereas the binding of the first $Mg^{2+}$ is sufficient for the start of the reaction (i.e., formation of the joint molecule). Thus, RecA drives these two processes in distinct manners. Binding of two $Mg^{2+}$ ions by RecA is not incompatible with the results of Cox and colleagues, who showed that RecA with a shorter deletion of the acidic tail (five amino acids) still exhibits some $Mg^{2+}$ dependence (17). Because the deletion they studied was so short, one of the $Mg^{2+}$-binding sites was likely to be retained. Our observations indicate that the role of RecA in the strand exchange reaction is not simply to bring two DNA molecules close to each other, but also to stimulate another step of the reaction, probably by actively promoting the displacement or repositioning of DNA strands. RecA differs from some polymers and surfaces that promote DNA strand exchange reactions by simply bringing two DNAs close to each other in a hydrophobic environment and relying on the characteristics of the DNA to execute strand exchange (39). In future work, we will investigate more precisely which step of the reaction is affected by the second $Mg^{2+}$ binding, and how this effect occurs.

An issue that we hope to address in future is how the binding of the second $Mg^{2+}$ stimulates progression of the strand

exchange reaction. Our results from this study indicate that some change in the subunit/subunit or domain/domain contacts of RecA occurs upon binding of two $Mg^{2+}$ ions or deletion of the acidic tail. Such a structural change is probably important for progression of the strand exchange reaction. Our simulation analysis suggests that $Mg^{2+}$ causes a change in the subunit/subunit contacts of RecA. Notably in this regard, Yu and Egelman showed by electron microscopic analysis that deletion of the acidic tail affects the structure of the RecA/DNA filament and increases its flexibility ([40]). Accordingly, we should also investigate whether the large destabilization of RecA upon binding of $Mg^{2+}$ is important for the strand exchange reaction by facilitating some key conformational change of the protein. Our preliminary analysis showed that the thermal stability of human Rad51 is also decreased by $Ca^{2+}$, the divalent ion that stimulates this protein (data not shown).

Another question is whether the acidic tail plays some biological role by exercising a negative effect on the strand exchange reaction. We wonder whether the tail has a regulatory function, or instead simply stabilizes RecA to increase its lifespan in the cells, in which case the negative effect would be just a byproduct. Stimulation of the strand exchange reaction by divalent ions has been reported for other eukaryotic recombinases (e.g., Rad51 and Dmc1) ([41,42]). Mazin and colleagues found that the stimulation mode of Dmc1 by $Ca^{2+}$ differs from that of Rad51 ([42]), suggesting the presence of more than two activation modes. This feature may be a general characteristic of recombinases. It will be interesting to determine whether the activation of Dmc1 and Rad51 by $Ca^{2+}$ occurs by a similar mechanism to that of RecA, in which metal ions bind to a part of the protein, hampering the interaction with other parts, and this inhibition is abolished by ion binding. Such a similarity would indicate that the inhibitory effect of the tail on the strand exchange reaction, or its regulation, is physiologically significant.

## SUPPLEMENTARY DATA

Supplementary Data are available at NAR online.

## REFERENCES

1. Michel,B., Flores,M.J., Viguera,E., Grompone,G., Seigneur,M. and Bidnenko,V. (2001) Rescue of arrested replication forks by homologous recombination. *Proc. Natl. Acad. Sci. U.S.A.*, **98**, 8181–8188.
2. Lusetti,S.L. and Cox,M.M. (2002) The bacterial RecA protein and the recombinational DNA repair of stalled replication forks. *Annu. Rev. Biochem.*, **71**, 71–100.
3. Krejci,L., Altmannova,V., Spirek,M. and Zhao,X. (2012) Homologous recombination and its regulation. *Nucleic Acids Res.*, **40**, 5795–5818.
4. Krzywinska,E., Krzywinski,J. and Schorey,J.S. (2004) Naturally occurring horizontal gene transfer and homologous recombination in Mycobacterium. *Microbiology*, **150**, 1707–1712.
5. Thomas,K.R. and Capecchi,M.R. (1986) Introduction of homologous DNA sequences into mammalian cells induces mutations in the cognate gene. *Nature (London)*, **324**, 34.
6. Bishop,A.J.R. and Schiest,R.H. (2002) Homologous recombination and its role in carcinogenesis. *J. Biomed. Biotechnol.*, **2**, 75–85.
7. Helleday,T. (2010) Homologous recombination in cancer development, treatment and development of drug resistance. *Carcinogenesis*, **31**, 955–960.
8. Carson,A., Wang,Z., Xiao,X. and Khan,S.A. (2005) A DNA recombination-based approach to eliminate papillomavirus infection. *Gene Ther.*, **12**, 534–540.
9. Cox,M.M. and Lehman,I.R. (1982) recA protein-promoted DNA strand exchange. *J. Biol. Chem.*, **257**, 8523–8532.
10. Shibata,T., Das Gupta,C., Cunningham,R.P. and Radding,C.M. (1979) Purified Escherichia coli recA protein catalyzes homologous pairing of superhelical DNA and single-stranded fragments. *Proc. Natl. Acad. Sci. U.S.A.*, **76**, 1638–1642.
11. Takahashi,M. (1989) Analysis of DNA-RecA protein interactions involving the protein self-association reaction. *J. Biol. Chem.*, **264**, 288–295.
12. Prévost,C. and Takahashi,M. (2003) Geometry of the DNA strands within the RecA nucleofilament: role in homologous recombination. *Q. Rev. Biophys.*, **36**, 429–453.
13. Candelli,A., Modesti,M., Peterman,E.J.G. and Wuite,G.J.L. (2013) Single-molecule views on homologous recombination. *Q. Rev. Biophys.*, **46**, 323–348.
14. Prentiss,M., Prevost,C. and Danilowicz,C. (2015) Structure/function relationships in RecA protein-mediated homology recognition and strand exchange. *Cri. Rev. Biochem. Mol. Biol.*, **50**, 1–24.
15. Bell,J.C. and Kowalczykowski,S.C. (2016) RecA: Regulation and mechanism of a molecular search engine. *Trends Biochem. Sci.*, **41**, 491–507.
16. Roman,L.J. and Kowalczykowski,S.C. (1986) Relationship of the physical and enzymic properties of Escherichia coli recA protein to its strand exchange activity. *Biochemistry*, **25**, 7375–7385.
17. Lusetti,S.L., Shaw,J.J. and Cox,M.M. (2003) Magnesium ion-dependent activation of the RecA protein involves the C terminus. *J. Biol. Chem.*, **278**, 16381–16388.
18. Gueroult,M., Boittin,O., Mauffret,O., Etchebest,C. and Hartmann,B. (2012) $Mg^{2+}$ in the major groove modulates B-DNA structure and dynamics. *PlosOne* **7**, e41704.
19. Pantoliano,M.W., Petrella,E.C., Kwasnoski,J.D., Lobanov,V.S., Myslik,J., Graf,E., Carver,T., Asel,E., Springer,B.A., Lane,P. *et al.* (2001) High-density miniaturized thermal shift assays as a general strategy for drug discovery. *J. Biomol. Screen.*, **6**, 429–440.
20. Lakowicz,J.R. (1999) *Principles of Fluorescence Spectroscopy*. 2nd edn. Plenium Publishers, NY.
21. Nordén,B., Rodger,A. and Dafforn,T. (2010) *Linear Dichroism and Circular Dichroism: A Textbook on Polarized-Light Spectroscopy*. Royal Society of Chemistry, Oxford.
22. Ganem,B., Li,Y. and Henion,J. (1991) Detection of noncovalent receptor ligand complexes by mass-spectrometry. *J. Am. Chem. Soc.*, **113**, 6294–6296.
23. Ishii,K., Noda,M. and Uchiyama,S. (2016) Mass spectrometric analysis of protein–ligand interactions. *Biophys. Physicobiol.*, **13**, 87–95.
24. Lee,C.D., Sun,H.C., Hu,S.M., Chiu,C.F., Homhuan,A., Liang,S.M., Leng,C.H. and Wang,T.F. (2008) An improved SUMO fusion protein

system for effective production of native proteins. *Protein Sci.*, **17**, 1241–1248.

25. Morrical,S.W. and Cox,M.M. (1985) Light scattering studies of the recA protein of Escherichia coli: relationship between free recA filaments and the recA/ssDNA complex. *Biochemistry*, **24**, 760–767.

26. Ishii,K., Noda,M., Yagi,H., Thammaporn,R., Seetaha,S., Satoh,T., Kato,K. and Uchiyama,S. (2015) Disassembly of the self-assembled, double-ring structure of proteasome α7 homo-tetradecamer by α6. *Sci. Rep.*, **5**, 18167.

27. Chen,Z., Yang,H. and Pavletich,N.P. (2008) Mechanism of homologous recombination from the RecA-ssDNA/dsDNA structures. *Nature*, **453**, 489–494.

28. Phillips,J.C., Braun,R., Wang,W., Gumbart,J., Tajkhorshid,E., Villa,E., Chipot,C., Skeel,R.D., Kale,L. and Schulten,K. (2005) Scalable molecular dynamics with NAMD. *J. Comp. Chem.*, **26**, 1781–1802.

29. MacKerell,A.D., Feig,M. and Brooks,C.L. (2004) Extending the treatment of backbone energetics in protein force fields: Limitations of gas-phase quantum mechanics in reproducing protein conformational distributions in molecular dynamics simulations. *J. Comp. Chem.*, **25**, 1400–1415.

30. Saladin,A., Fiorucci,S., Poulain,P., Prévost,C. and Zacharias,M. (2009) PTools: an open source molecular docking library. *BMC Struct. Biol.*, **9**, 27–38.

31. Haruta,N., Kurokawa,Y., Murayama,Y., Akamatsu,Y., Unzai,S., Tsutsui,Y. and Iwasaki,H. (2006) The Swi5-Sfr1 complex stimulates Rhp51/Rad51- and Dmc1-mediated DNA strand exchange *in vitro*. *Nat. Struct. Mol. Biol.*, **13**, 823–830.

32. Ito,K., Murayama,Y., Takahashi,M. and Iwasaki,H. (2018) Two three-strand intermediates are processed during Rad51-driven DNA strand exchange. *Nat. Struct. Mol. Biol.*, **25**, 29–36.

33. Bazemore,L.R., Takahashi,M. and Radding,C.M. (1997) Kinetic analysis of pairing and strand exchange catalyzed by RecA. Detection by fluorescence energy transfer. *J. Biol. Chem.*, **272**, 14672–14682.

34. Story,R.M., Weber,I.T. and Steitz,T.A. (1992). The structure of the E. coli recA protein monomer and polymer. *Nature*, **355**, 318–325.

35. Sancar,A., Stachelek,C., Konigsberg,W. and Rupp,W.D. (1980) Sequences of the recA gene and protein. *Proc. Natl. Acad. Sci. U.S.A.*, **77**, 2611–2615.

36. Daniel,J.M., Friess,S.D., Rajagopalan,S., Wendt,S. and Zenobi,R. (2002) Quantitative determination of noncovalent binding interactions using soft ionization mass spectrometry. *Int. J. Mass Spectrom.*, **216**, 1–27.

37. Aihara,H., Ito,Y., Kurumizaka,H., Terada,T., Yokoyama,S. and Shibata,T. (1997) An interaction between a specified surface of the C-terminal domain of RecA protein and double-stranded DNA for homologous pairing. *J. Mol. Biol.*, **274**, 213–221.

38. Yang,D., Boyer,B., Prévost,C., Danilowicz,C. and Prentiss,M. (2015) Integrating multi-scale data on homologous recombination into a new recognition mechanism based on simulations of the RecA-ssDNA/dsDNA structure. *Nucleic Acids Res.*, **43**, 10251–10263.

39. Feng,B., Westerlund,F. and Norden,B. (2015) Evidence for hydrophobic catalysis of DNA strand exchange. *Chem. Commun.*, **51**, 7390–7392.

40. Yu,X. and Egelman,E.H. (1991) Removal of the RecA C-terminus results in a conformational change in the RecA-DNA filament. *J. Struct. Biol.*, **106**, 243–254.

41. Bugreev,D.V. and Mazin,A.V. (2004) $Ca^{2+}$ activates human homologous recombination protein Rad51 by modulating its ATPase activity. *Proc. Natl. Acad. Sci. U.S.A.*, **101**, 9988–9993.

42. Bugreev,D.V., Golub,E.I., Stasiak,A.Z., Stasiak,A. and Mazin,A.V. (2005) Activation of human meiosis-specific recombinase Dmc1 by $Ca^{2+}$. *J. Biol. Chem.*, **280**, 26886–26895.